Soft Matter

Low solid content mouldable chitin physical hydrogel prepared by atypical rupture-free swelling

Journal:	*Soft Matter*
Manuscript ID	SM-ART-11-2023-001542.R1
Article Type:	Paper
Date Submitted by the Author:	20-Dec-2023
Complete List of Authors:	Kaku, Yuto; The University of Tokyo, Agricultural and Life Sciences Okada, Satoshi; Japan Agency for Marine-Earth Science and Technology, Institute for Extra-cutting-edge Science and Technology Avant-garde Research Fujisawa, Shuji; The university of Tokyo, Department of Biomaterial Sciences Saito, Tsuguyuki; The University of Tokyo, Agricultural and Life Sciences Isobe, Noriyuki; Japan Agency for Marine-Earth Science and Technology, Research Institute for Marine Resources Utilization

ARTICLE

Low solid content mouldable chitin physical hydrogel prepared by atypical rupture-free swelling

Yuto Kaku,[a,b] Satoshi Okada,[c] Shuji Fujisawa,[a] Tsuguyuki Saito,[a] and Noriyuki Isobe *[b,a]

Received 00th January 20xx,
Accepted 00th January 20xx

DOI: 10.1039/x0xx00000x

Received 00th January 20xx,
Accepted 00th January 20xx

DOI: 10.1039/x0xx00000x

In this study, the atypical swelling gelation of chitin physical hydrogels was investigated. Only by tuning the amount of the *N*-acetylation reagent, the degree of acetylation varied and mouldable chitin hydrogels with a wide variety of gel concentrations (0.2–6.4 wt%) were obtained. In response to the gel concentration, the mechanical properties ranged from swollen soft gels to shrunken rigid gels (compressive moduli of 4–310 kPa). The thus-prepared chitin hydrogels, which were composed of only chitin and water, exhibited high transparency and integrity. The swelling gelation of chitin physical hydrogels was achieved owing to both the positive charges of the amino groups inducing the osmotic pressure and the toughness of the crystalline nanofibrous network structure of the chitin hydrogels that endured the large volume change. These previously unnoticed advantageous aspects of chitin have pioneered a novel region of swellable physical gels that has been exclusive to chemical gels so far.

Introduction

Gels are composed of sub-nanoscale or nanoscale architectures, such as interconnected polymer chains, nanofibres, and nanofilaments. Depending on the nature of the interconnection, the so-called cross-linking, gels are classified into chemical or physical gels. Chemical gels are prepared by covalently cross-linking polymer molecules with chemical reagents, while physical gels are obtained by physical cross-linking, such as molecular entanglement and formation of crystalline region that act as a junction zone.[1] Physical gels, such as agar and gelatin hydrogels, are advantageous in terms of the absence of chemical cross-linking reagents, thereby making them biocompatible and environmentally friendly.[2–6]

Owing to the gelation mechanism of physical gels, the distance between the molecular chains becomes closer to some extent during gelation, and the thus-obtained physical gels generally exhibit shrinking gelation, although the degree of shrinkage varies. Consequently, the resulting physical gels are more condensed (generally more than 1 wt% of solid concentration) compared with chemical gels. To obtain physical gels with low solid content, swelling of once-prepared gels can be one option. However, swelling of physical gels is impossible because the gel is ruptured owing to the mechanical brittleness of physical gels. It is commonly understood that swelling only occurs in chemical gels.[7] Many studies have reported swellable

[a] *Department of Biomaterial Sciences, Graduate School of Agricultural and Life Sciences, The University of Tokyo, 1-1-1 Yayoi, Bunkyo-ku, Tokyo 113-8657, Japan*
[b] *Biogeochemistry Research Center, Research Institute for Marine Resources Utilization, Japan Agency for Marine-Earth Science and Technology (JAMSTEC), 2-15 Natsushima-cho, Yokosuka, Kanagawa 237-0061, Japan.*
[c] *Institute for Extra-cutting-edge Science and Technology Avant-garde Research (X-STAR), Japan Agency for Marine-Earth Science and Technology (JAMSTEC), 2-15 Natsushima-cho, Yokosuka, Kanagawa 237-0061, Japan*
Electronic Supplementary Information (ESI) available: [details of any supplementary information available should be included here]. See DOI: 10.1039/x0xx00000x

chemical gels and their useful functions as soft materials.[8–12] A discontinuous volume change called a volume phase transition is caused by the presence of positive or negative charges in hydrogels.[13,14] To overcome this drawback and induce swelling gelation in physical gels, two conditions are necessary: (i) the gel needs to be positively or negatively charged to induce osmotic pressure and (ii) the gel needs to be sufficiently deformable to endure the volume change.[15]

Chitin is one of the best candidates for swelling gelation. Chitin, the second most abundant polysaccharide, is an unbranched polymer of *N*-acetylglucosamine that forms crystalline nanofibres or nanorods in the native state.[16] Owing to the excellent mechanical properties of crystalline chitin,[17,18] chitin is used as the skeletal building block in crustaceans,[19,20] insects,[21,22] fungi,[23] and marine sponges.[24–29] The *N*-acetyl groups of chitin can be removed by alkaline treatment, and when the degree of acetylation is less than 60%, the deacetylated derivative is called chitosan. Upon deacetylation, the amino groups are exposed and bear positive charges under acidic conditions. Therefore, partially deacetylated chitin can serve as a building block for swellable physical hydrogels owing to its positive charges under acidic conditions and remarkable mechanical properties.

Among the wide variety of chitinous materials, the *N*-acetylated chitosan hydrogel developed by Hirano and co-workers[30–32] is a promising candidate for swelling materials. Briefly, chitosan was dissolved in acidic alcohol solution, and upon subsequent *N*-acetylation, chitosan became chitin, which was no longer soluble in acidic alcohol solution, resulting in the formation of a chitin physical gel. Although the chemical features of *N*-acetylated chitosan hydrogel have been investigated,[33–37] it has not been fully characterised as a robust bulk material despite its high integrity, transparency, and thermal stability. This mainly arises from the difficulty in the preparation of a robust bulky gel specimen because the gelation of the chitin hydrogel immediately starts during the mixing of the *N*-acetylation reagent, making it difficult to prepare a homogeneous and mouldable chitin hydrogel.

Recently, a new process to obtain mouldable chitin hydrogels based on the above gelation method has been reported.[38] By mixing the *N*-acetylation reagent at low temperature, the gelation speed slowed down and the moulding of the chitin physical hydrogel with high mechanical toughness was successful. This novel strategy paved the way for the preparation of mouldable swellable physical gels. By tuning the amount of the *N*-acetylation reagent, it is possible to control the amount of positively charged amino groups, leading to swelling gelation. Here, we show the successful preparation of chitin physical hydrogels that underwent swelling while maintaining their shape, and the structure–property relationships of the prepared hydrogels were investigated. The finding of this study will open up an unexplored area of mouldable swellable physical gels that has previously been exclusive to chemical gels.

Experimental

Materials

Acetic acid (99% purity), acetic anhydride (Ac_2O, 97% purity), hydrochloric acid (1 M), sodium hydroxide (97% purity), methanol (99.8% purity), and chitosan powder (chitosan 100, molecular weight = 1.3×10^6)[39] were purchased from Fujifilm Wako Pure Chemical Corporation (Japan). The degree of acetylation (DA) of the chitosan powder was measured to be ~20%. Deionised water was used throughout the study.

Preparation of the chitin hydrogel

The chitin hydrogel was prepared according to a previously reported method[38] with a minor modification (Scheme 1). Chitosan powder (fixed to 0.75 g except for Fig. 1c) was dissolved in acetic acid (1.5 mL)/water (13.5 mL), followed by dilution with methanol (60 mL). The chitosan solution was cooled to −12 °C and a desired amount of Ac_2O was added. After complete mixing, the mixture was poured into cylindrical moulds (5 mL per mould) and left at room temperature to ensure complete gelation. The size of the mould was 2.8 cm in height and 1.8 cm in diameter. The gelation completes within 4 h and the obtained alcogels were removed from the moulds. The chitin alcogels at this stage showed a slight shrinkage with syneresis or no volume change (Fig. S1). After thorough washing with water until the wastewater showed the same conductivity as deionised water, chitin hydrogels were obtained (Scheme 1). Several hydrogels collapsed during preparation and measurement of their size was not feasible. Therefore, the gel volume (V) was measured gravimetrically according to the following equation:

$$V = \frac{w_\mathrm{d}}{\rho_\mathrm{c}} + \frac{w_\mathrm{h} - w_\mathrm{d}}{\rho_\mathrm{w}}$$

where ρ_c, ρ_w, w_h, and w_d are the density of chitin (1.425 g/cm^3),[40] density of water (1.0 g/cm^3), weight of the chitin hydrogel, and weight of the gel oven-dried at 105 °C for 3 h, respectively. The average of three specimens was taken as the final gel volume. The validity of the above equation was investigated beforehand using robust chitin hydrogels, and the volumes calculated with the above equation corresponded well (R^2 = 0.997) with those calculated by measuring their sizes (Fig. S2). The volume change was calculated by dividing the gel volume (V) by the initial added amount (5 mL).

Determination of the degree of acetylation

The DA values of the chitin hydrogels were measured by conductivity titration. The hydrogels were freeze-dried, and the dried gels were stirred in water overnight. They were then adjusted to pH 10 using 1 M sodium hydroxide solution, and subsequently to pH 3 using 1 M hydrochloric acid. After the pre-treatment, 0.05 M sodium hydroxide solution was added to the samples at a constant speed of 0.1 mL/min, and the pH and conductivity curves were obtained. To ensure the accuracy, the DA values were measured every time the chitin hydrogels were prepared. This is due to that the DA values and the volumes of the hydrogels varied even when exactly the same preparative condition was applied, specifically in the boundary condition between swelling and shrinking (see the range indicated with the gradient in Fig. 1c).

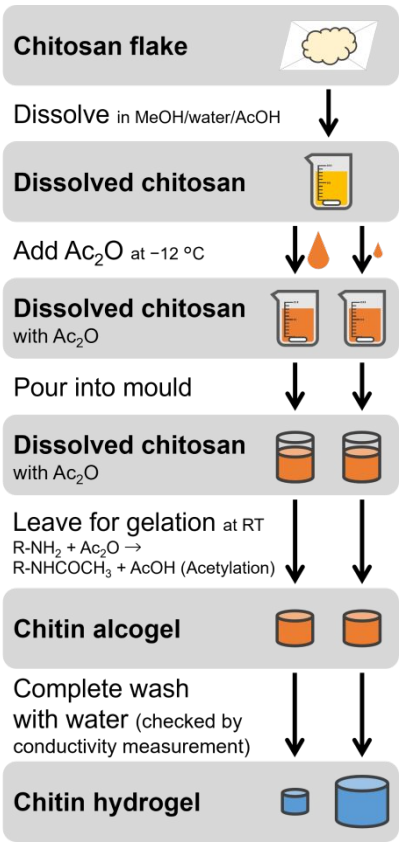

Scheme 1. Preparation protocol of chitin hydrogels. R in the scheme represents $C_6H_9O_4$.

Mechanical property analysis

To investigate the mechanical properties of the chitin hydrogels, compression tests were performed at 23 °C and 50% relative humidity using a compression instrument (EZ-SX, Shimadzu Corporation, Japan) with a 500 N load cell at a constant compression velocity of 1.0 mm/min, which corresponded to the flexural strain from 3 to 10 %, depending on the size of the sample specimen. Based on the comparative compression tests with the velocity of 1.0 mm/min and the compression strain rate of 5%/min (Fig. S3), the compression velocity was considered to be sufficiently slow in this study. The compressive modulus was calculated from the slope of the initial elastic region of the stress-strain curve until 5% strain on the assumption that the cross-sectional area of the sample was constant during the test. The size of the samples was carefully measured using a digital calliper (DT-150, Niigata Seiki Co., Ltd., Japan). The shape of the samples was cylindrical with approximately 1–3 cm in diameter, and the reported values are the average of three specimens.

X-ray diffraction analysis

Small-angle X-ray scattering (SAXS) and wide-angle X-ray diffraction (WAXD) were performed with synchrotron radiation at the BL40B2 beamline of SPring-8 (Hyogo, Japan). The chitin hydrogels (solid contents of 0.25, 1.1, and 6.4 wt%) were prepared 1 day before the measurements and kept hydrated in water at ambient temperature during transport to the beamline. It should be noted that slight condensation of the hydrogel was likely because of unavoidable evaporation of water during handling or syneresis induced by the temperature change during transportation. The wet samples were packed in a glass capillary at the beamline and X-rays (10 keV for 10 s for SAXS and 22 keV for 100 s for WAXD) was irradiated. The distance between the sample and the imaging plate (3190.33 mm for SAXS and 95.33 mm for WAXD) was calibrated using silver behenate powder (d = 5.838 nm).[41]

Cryo-scanning electron microscopy observation

The cryo-scanning electron microscopy (cryo-SEM) observations were performed with a dual beam focused ion beam/scanning electron microscope (Helios G4 UX, Thermo Fisher Scientific Inc., USA) equipped with a cryogenic stage (PP3010T, Quorum Technologies Ltd, UK). The samples were cut to approximately 0.5 mm × 0.5 mm × 10 mm by a scalpel in water. The gel was inserted through the internal cavity of a pair of hollow brass rivets (bore = 1.0 mm) whose upper ends were in contact. The rivets were rapidly cooled in slush nitrogen (approximately −210 °C), mounted on a transfer shuttle, and the top rivet was removed to expose the cross section of the gel. The rivet was vacuum transferred to a vacuum preparation stage (approximately 2×10^{-4} Pa) and heated to −80 °C for 10 min to sublime water. The sample was transferred to a SEM chamber (approximately −160 °C) and observed at a landing voltage of 1 kV while applying 50 V of anti-bias on the sample. To mitigate the effect of conductive coating, the observation was performed without a coating process as in the previous study.[38]

Results and discussion

Swelling or shrinking gelation of the chitin physical hydrogels

The chitin gels exhibited DA-dependent swelling or shrinking during washing, leading to highly swollen soft hydrogels or shrunken rigid hydrogels, respectively. Photographs of the representative moulded swollen and shrunken chitin hydrogels are shown in Fig. 1a. The DA values of the swollen (volume change = 351%), unchanged (volume change = 107%), and shrunken (volume change = 17%) chitin hydrogels were 83%, 86%, and 99%, respectively. The moulded hydrogels were bulky and sufficiently robust to be grabbed by the hand. One can clearly read the printed words through the hydrogels, confirming their high transparency.

The gelation by *N*-acetylation originates from the insolubilisation of *N*-acetylated chitosan, namely, chitin. The chitosan molecules dissolved in acidic alcohol become insoluble upon *N*-acetylation, and the chitin molecules form crystalline fibrous networks, serving as junction zones in the gel structure.[38] Therefore, the DA value is an important parameter to determine the mechanical properties of the resultant gel. The chitin gels shrank under sufficient *N*-acetylation (DA > 95%), and a drastic increase of the gel volume was observed as the DA value decreased (Fig. 1b). The most swollen one (DA = 80.8%) bulked up to 463% of the initial size before water washing, whereas the most shrunk one (DA = 99.4%) reduced its volume to 16%. When

the DA value was less than 80%, the resultant hydrogels became too fragile and collapsed, making it impossible to measure their weights (Fig. S4). Between 85% and 95% of DA, the data points of volume change were scattered. This is because near the boundary condition between swelling and shrinking several uncontrollable factors such as slight difference in the initial sample amount, freshness and injection speed of Ac_2O, mixing speed, and temperature and humidity during gelation can highly affect the results.

The phase diagram based on the volume change of the chitin gels with respect to the initial concentration of chitosan and the DA value is shown in Fig. 1c. Depending on the preparation conditions, the gel state can be divided into the collapsed state, the swollen state, and the shrunken state. The boundary of the DA between no gelation (the collapsed state) and gelation (the swollen or shrunken state) showed a monotonic decrease with increasing initial chitosan concentration. This is probably because at higher initial chitosan concentration, the chitosan molecules were located closer to each other, and even with less *N*-acetylation, a sufficient number of physically cross-linked junction zones were formed, and the hydrogel mechanically endured the expansion without rupture. In contrast, the boundary of the DA between the swollen and shrunken states showed a monotonic increase with increasing initial chitosan concentration. Generally, the swelling of a gel is driven by the osmotic pressure.[13,14] In the present study, the swelling was induced by the osmotic pressure driven by the positive charges originating from the NH_3^+ groups at the C2 position of the unacetylated monomeric units of chitin, namely, glucosamine. Therefore, this trend can be explained by, despite the small charge per molecule (namely, high DA), the charge density was sufficiently high for swelling because a large number of molecules were present. Consequently, the swelling gelation of the chitin hydrogel was balanced out by the mechanical properties of the network structure in the chitin gel and the osmotic pressure induced by the NH_3^+ groups of the unacetylated residues of chitin, as in the case of chemical gels.[13,14]

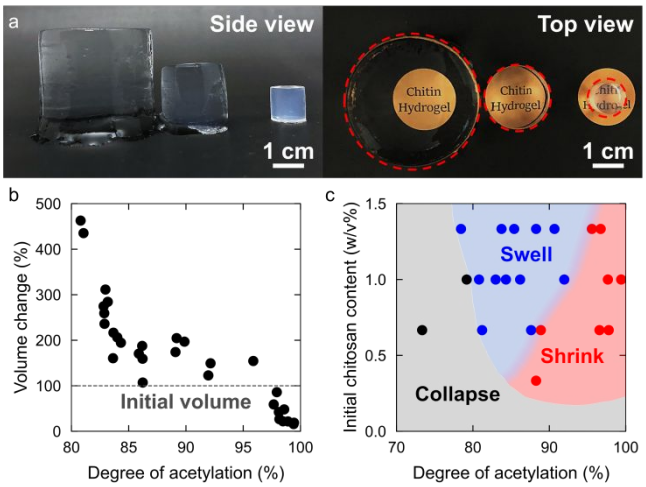

Fig. 1. (a) Photographs of the representative swollen, unchanged, and shrunken chitin hydrogels (the DA values were 83%, 86%, and 99%, respectively). The orange circles represent the size of the mould used for the hydrogel preparation. (b) Volume change of the chitin hydrogels prepared under various degrees of acetylation. The dashed line represents the initial volume of the mould used for the gelation. (c) Phase diagram of collapsing, swelling, and shrinking gelation of chitin hydrogels with different initial chitosan contents and degrees of acetylation. The initial chitosan amount was 0.25, 0.5, 0.75, and 1.0 g.

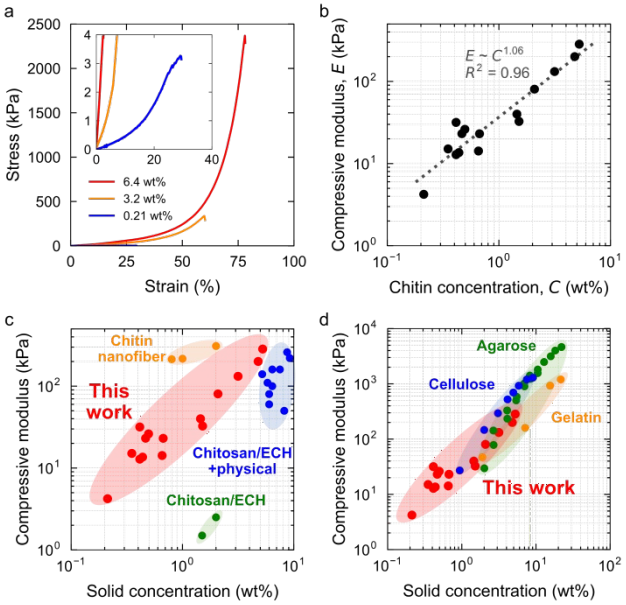

Fig. 2. (a) Stress–strain curves of the chitin hydrogels with different gel concentrations. (b) Compressive moduli of the chitin hydrogels plotted against the chitin concentrations. (c) Comparison of the compressive moduli in this study with those of representative chitin-based hydrogels: chitin nanofiber-based hydrogels (chitin nanofiber),[46] chemical chitosan hydrogels cross-linked with epichlorohydrin (ECH) (chitosan/ECH),[47] chemical chitin hydrogels cross-linked with ECH followed by physical gelation (chitosan/ECH + physical),[43] and physical chitin hydrogels (this work). (d) Comparison of the compressive moduli of the hydrogels in this study with those of different polysaccharide-based hydrogels: cellulose,[48] agarose,[45] gelatin,[49] and chitin hydrogels (this work).

Mechanical properties of the chitin hydrogels

One of the remarkable features of the chitin hydrogels obtained in this study was the wide range of gel concentrations from 0.21 to 6.4 wt%. Therefore, the chitin hydrogels exhibited a broad range of mechanical properties depending on the gel concentration. The representative compressive stress–strain curves of the chitin hydrogels are shown in Fig. 2a. The compressive strength of the hydrogel was dependent on the gel concentration (Fig. S5) and at the highest gel concentration it reached over 2 MPa at 80% strain. This value is comparable with those of known chitin hydrogels with similar or even higher gel concentrations, where chemical or physical cross-linking reagents were introduced.[42,43] In contrast, the compressive strength of the hydrogel with the lowest gel concentration was approximately 3 kPa, which was three orders of magnitude less than that of the highest compressive strength. It should be noted that this highly soft swollen chitin hydrogel did not

rupture at 30% strain, indicating that the tough nature of the chitin hydrogel was maintained even in the swollen state.

The compressive moduli of the chitin hydrogels (Table S1) were calculated from the elastic region of stress–strain curves (Fig. 2a), and they are shown with respect to the gel concentration in Fig. 2b. Generally, the compressive modulus of hydrogels follows a power law of the concentration of the cross-linking molecules.[44,45] In this study, a strong correlation ($E \sim C^{1.06}$, R^2 = 0.96) between the gel concentration and compressive modulus was observed despite the difference in the DA values. Therefore, it can be considered that the number of junction zones, namely, the chitin concentration, made a dominant contribution to the compressive modulus. Although the compressive moduli of the chitin hydrogels were not as high as those made of highly crystalline chitin nanofibres (Fig. 2c), they covered a wide range of 4–310 kPa, which is broader than those of other chitin-based or polysaccharide-based hydrogels (Fig. 2c and d). It should be emphasised that this tuneable diversity of the mechanical properties arises from only the change in the added amount of Ac_2O for *N*-acetylation.

Structure–property relationship

The structure–property relationship of the swollen and shrunken chitin hydrogels was elucidated. First, the network structures of the chitin hydrogels were investigated by cryo-SEM (Fig. 3). Regardless of swelling or shrinking, nanofibrous network structures (diameter of approximately 10 nm) were found to be the principal building blocks. This explains the high transparency of the chitin hydrogels, as in the previous study.[38] While the shrunken gel showed a highly dense and homogeneous network structure (Fig. 3a), the swollen gel showed a sparse network structure along with a partly inhomogeneous cell-like structure (Fig. 3b), which was due to the unavoidable ice crystal formation during high-pressure freezing.[50–52] This sparse network structure in the swollen gel was formed by decreasing the DA value, where the amount of positive charge increased and more osmotic pressure was introduced, as mentioned above. Therefore, the nanoarchitecture of the chitin hydrogel was controllable by only changing the added amount of Ac_2O for *N*-acetylation.

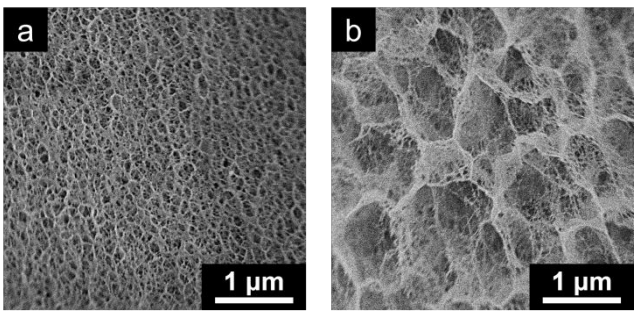

Fig. 3. Cryo-SEM images of the (a) shrunken (volume change = 17%) and (b) swollen (volume change = 200%) chitin hydrogels.

The fibrous network structures of the swollen and shrunken chitin hydrogels were analysed by X-ray diffraction/scattering measurements (Fig. 4). In the SAXS profiles, the swollen, unchanged, and shrunken chitin hydrogels (volume changes of 386%, 100%, and 16%, respectively) showed striking differences in the lower *q* region (Fig. 4a). To focus on this difference, the SAXS profiles were converted to Kratky plots (Fig. 4b). For the swollen chitin hydrogel (0.25 wt%), a broad peak centred at approximately q = 0.05 $Å^{-1}$ was observed. This peak was likely to originate from the surface of the fibrous network structure of the chitin hydrogel because the slope of log-log plots in Fig. 4a was close to the power of −4.[53] Upon an increase of the solid content, namely, for the shrunken gel, a new broad peak centred at q = 0.02 $Å^{-1}$ appeared. This peak originated from the correlation length of the fibrous network structure of the chitin hydrogel, namely, the fibre–fibre distance (d = 31.4 nm). For the shrunken hydrogel, the fibre–fibre distance was sufficiently short to be detected in the current q region.[54] This result is in good agreement with the cryo-SEM image (fibre–fibre distance = approximately 30–100 nm) showing a densely packed fibrous network structure (Fig. 3a). All of the WAXD profiles of the chitin hydrogels showed clear peaks of α-chitin even in the hydrated state (Fig. 4c). Although how much crystalline region existed in the chitin hydrogels, or crystallinity index, was unknown due to the strong scattering of water, all the chitin hydrogels, irrespective of swollen or shrunken gel, contained crystalline components. This indicated that the chitin gels underwent swelling or shrinking without affecting the primary architecture, namely, the nanofibrous network of crystalline α-chitin.

Fig. 4. (a) SAXS profiles of the chitin hydrogels. The chitin

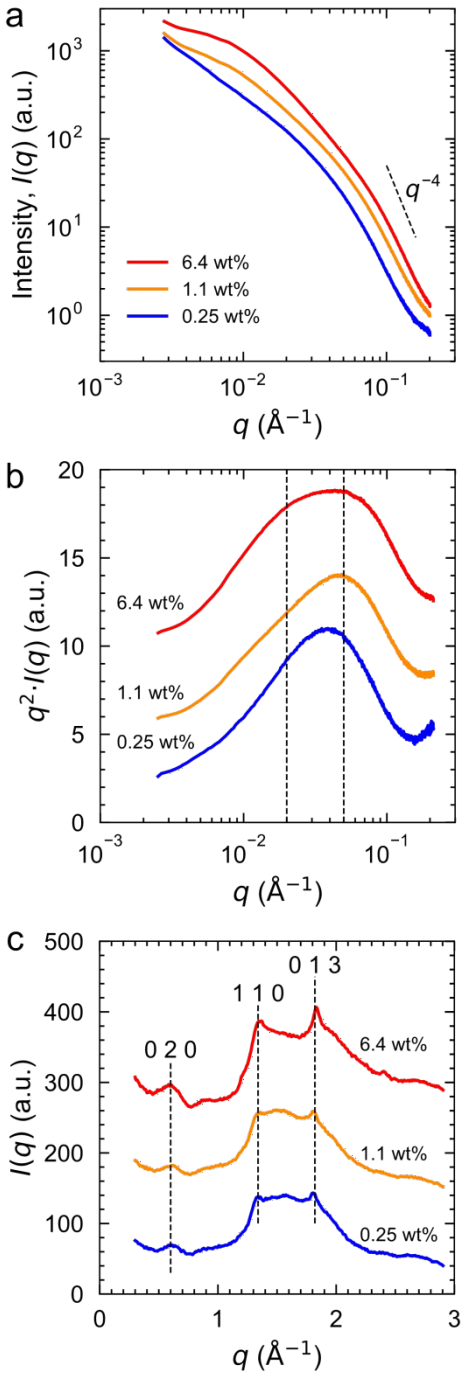

concentrations of the hydrogels are given in the figure. (b) Kratky plots of (a). For clarity, the intensities of the profiles were normalised to that of the 1.1 wt% chitin hydrogel and shifted vertically. (c) WAXD profiles of the chitin hydrogels. For clarity, the profiles were shifted vertically. The peaks were indexed according to the literature.[55]

According to the above findings, the osmotic pressure induced by the positive charge originating from the unacetylated NH_2 groups was assumed to play an essential role in the swelling or shrinking. Here, a quantitative analysis of the induced osmotic pressure was difficult because the pH in the gel gradually changes during the water washing process, and the exact ion concentration was unknown unlike previous reports.[56,57] Therefore, the driving force for swelling of the hydrogels was discussed based on the amount of the amino groups in this paper. To confirm the presence and quantify the amount of the remaining positively charged amino groups in the swollen hydrogels, conductivity titration of the shrunken and swollen chitin hydrogels was performed (Fig. 5). As described in the Experimental section, the measurement was performed just after the water washing of the hydrogels. For the shrunken chitin hydrogel, a linear increase in the conductivity value was observed (Fig. 5a), whereas two steps of the conductivity with different slopes (the line in light blue and blue) were observed for the swollen hydrogel (Fig. 5b). The existence of the first step, the deprotonation of the weak base, showed that the protonated amino groups remained even after water washing. Approximately 20% of the total amount of NH_2 groups in the hydrogel remained non-acetylated and protonated after washing (0.19 mmol/g NH_3^+ and 0.92 mmol/g total NH_2).

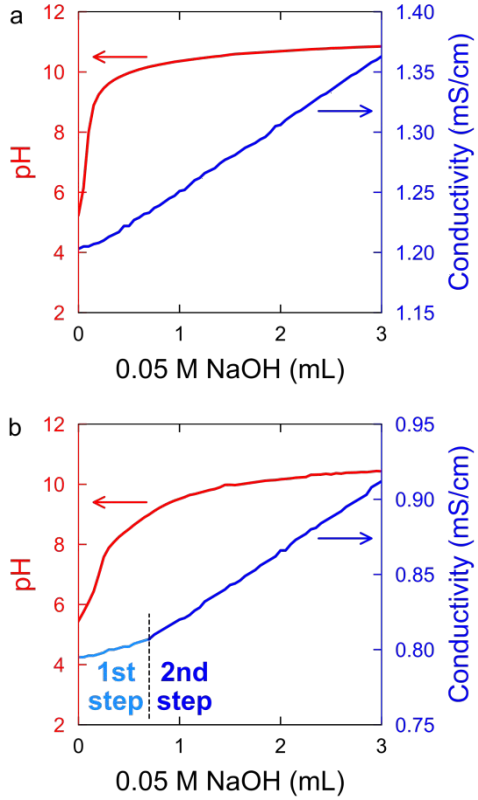

Fig. 5. Conductivity titration of the (a) shrunken (volume change = 16%, DA = 99.4) and (b) swollen (volume change = 275%, DA = 82.8) chitin hydrogels. Deprotonation of NH_3^+ was observed on the light blue line. The blue line reflected the injected NaOH.

Based on these results, the speculated mechanisms of the shrinking and swelling gelation of the chitin hydrogel are shown in Fig. 6. Chitosan is initially dissolved in acidic alcohol, in which the chitosan molecules are highly protonated. After sufficient *N*-acetylation (DA > 98%), the chitosan molecules become insoluble and a nanofibrous network structure composed of crystalline α-chitin is

formed, leading to gelation. After subsequent washing with water, shrinkage due to syneresis occurs. Similarly, upon insufficient *N*-acetylation (DA < 96%), the chitosan molecules become insoluble and a nanofibrous network structure composed of crystalline α-chitin is formed, leading to gelation. However, owing to the residual positively charged amino groups, the hydrogel swells through the subsequent washing with water by the osmotic pressure induced by the ionic strength of the remaining amino groups of the gel network, and the nanofibrous network structure composed of crystalline α-chitin endures large volume change, leading to the rupture-free swelling. At the boundary between swelling and shrinking gelation, the difference in the DA between shrunken and swollen gels was only 2%, suggesting that a small amount of the remaining amino groups played a decisive role in determining whether swelling or shrinking occurred. It should be noted that the extent of swelling fluctuates near the boundary between swelling and shrinking as described in the Experimental section and in the range indicated in the gradient in Fig. 1c.

Generally, physical gels are formed above overlapping concentrations, C^*, to have sufficient molecular entanglements. By using high molecular weight polymers, C^* can be lowered and physical gelation at low solid concentration can be possible. However, such polymers are hard to dissolve, and the resultant polymer solutions are extremely viscous, leading to the poor mouldability. Therefore, the preparation of mouldable chitin physical hydrogel with low solid content (~0.25 wt%) is only feasible with our unique approach, namely, swelling of physical gels.

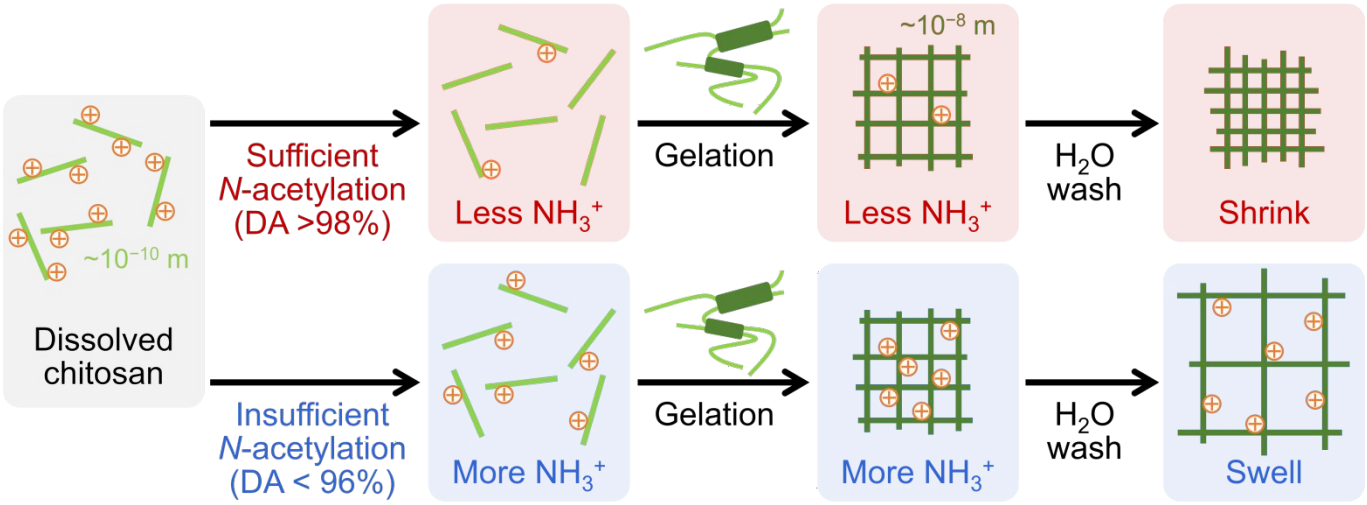

Fig. 6. Schematic illustration of the shrinking and swelling mechanisms of the chitin hydrogel.

ARTICLE

Conclusions

Chitin physical hydrogels have been investigated focusing on the anomalous rupture-free swelling after gelation. The obtained swollen chitin hydrogels were highly transparent, mould able, and sufficiently tough to be grabbed by the hands. the volume change of the chitin hydrogels originated from the remaining protonated amino groups, the amount of which depended on the added amount of the *N*-acetylating reagent. The obtained volume-controllable (from swollen to shrunken) chitin hydrogels exhibited a wide range of mechanical properties depending on the gel concentration. Swellable physical hydrogels were achieved using chitin owing to the positive charges and toughness of crystalline chitin. Focusing on these unique features, the chitin hydrogels in this study provide a novel platform for the utilisation of physical hydrogels.

Author Contributions

Yuto Kaku: conceptualisation, methodology, investigation, writing - original draft, writing - review & editing, funding acquisition. **Satoshi Okada**: methodology, investigation, writing - original draft. **Tsuguyuki Saito**: writing - review & editing, supervision, funding acquisition. **Shuji Fujisawa**: writing - original draft, writing - review & editing, supervision, funding acquisition. **Noriyuki Isobe**: conceptualisation, methodology, investigation, writing - original draft, writing - review & editing, supervision, funding acquisition.

Conflicts of interest

There are no conflicts to declare.

Acknowledgements

We thank Ms. Keiko Tanaka and Ms. Sachiko Kawada for technical assistance. The synchrotron radiation experiments were carried out at beamline BL40B2 of SPring-8 (proposal no. 2023A1134). This research was supported by Grants-in-Aid for Scientific Research (grant number JP22J12842 to Y.K., grant numbers JP23H02270 to S.F., grant numbers JP18K18188, JP22H03786, and JP22K19885 to N.I., and grant number JP21H04733 to T.S. from the Japan Society for the Promotion of Science (JSPS), and JST CREST (grant number JPMJCR22L3 to T. S. and S. F.) from the Japan Science and Technology Agency (JST), and the Research Program for Next Generation Young Scientists of the Network Joint Research Center for Materials and Devices: Dynamic Alliance for Open Innovation Bridging Human, Environment and Materials. (grant number 20225005 to Y.K.). This paper was partly based on the results obtained from projects, JPNP18016 and PJ-ID 20001845, commissioned by the New Energy and Industrial Technology Development Organization (NEDO).

References

1 M. Chelu and A. M. Musuc, *Gels*, 2023, **9**, 161.
2 M. N. Pinto, J. Martinez-Gonzalez, I. Chakraborty and P. K. Mascharak, *Inorg. Chem.*, 2018, **57**, 6692–6701.
3 T. Gürkan Polat, O. Duman and S. Tunç, *Colloids Surfaces A Physicochem. Eng. Asp.*, 2020, **602**, 124987.
4 Y. Deng, H. Wang, L. Zhang, Y. Li and S. Wei, *Mater. Lett.*, 2013, **104**, 8–12.
5 J. Lei, X. Li, S. Wang, L. Yuan, L. Ge, D. Li and C. Mu, *ACS Appl. Polym. Mater.*, 2019, **1**, 1350–1358.
6 G. V. N. Rathna, *J. Mater. Sci. Mater. Med.*, 2008, **19**, 2351–2358.
7 X. Shen, J. L. Shamshina, P. Berton, G. Gurau and R. D. Rogers, *Green Chem.*, 2015, **18**, 53–75.
8 W. Xue, S. Champ and M. B. Huglin, *Polymer (Guildf).*, 2001, **42**, 3665–3669.
9 X. Jiang, C. Li and Q. Han, *Polym. Bull.*, 2023, **80**, 1303–1320.
10 M. Liu and T. Guo, *J. Appl. Polym. Sci.*, 2001, **82**, 1515–1520.
11 D. K. Aktaş, G. A. Evingür and Ö. Pekcan, *J. Mater. Sci.*, 2007, **42**, 8481–8488.
12 H. B. Sonmez, K. Karadag and G. Onaran, *J. Appl. Polym. Sci.*, 2011, **122**, 1182–1189.
13 Toyoichi Tanaka, *Phys. Rev. Lett.*, 1978, **40**, 820–823.
14 T. Tanaka, S. T. Sun, I. Nishio, G. Swislow and A. Shah, *Ferroelectrics*, 1980, **30**, 97.
15 D. Jia and M. Muthukumar, *Gels*, 2021, **7**, 49.
16 M. V. Tsurkan, A. Voronkina, Y. Khrunyk, M. Wysokowski, I. Petrenko and H. Ehrlich, *Carbohydr. Polym.*, 2021, **252**, 117204.
17 T. Nishino, R. Matsui and K. Nakamae, *J. Polym. Sci. Part B Polym. Phys.*, 1999, **37**, 1191–1196.
18 Y. Ogawa, R. Hori, U. J. Kim and M. Wada, *Carbohydr. Polym.*, 2011, **83**, 1213–1217.
19 K. Shimahara and Y. Takiguchi, in *Methods in Enzymology*, 1988, vol. 161, pp. 417–423.
20 A. Percot, C. Viton and A. Domard, *Biomacromolecules*, 2003, **4**, 12–18.
21 M. D. Finke, *Zoo Biol.*, 2007, **26**, 105–115.
22 M. Kaya, S. Erdogan, A. Mol and T. Baran, *Int. J. Biol. Macromol.*, 2015, **72**, 797–805.

23 H. J. Blumenthal and S. Roseman, *J. Bacteriol.*, 1957, **74**, 222–224.
24 H. Ehrlich, M. Maldonado, K. Spindler, C. Eckert, T. Hanke, R. Born, C. Goebel, P. Simon, S. Heinemann and H. Worch, *J. Exp. Zool. Part B Mol. Dev. Evol.*, 2007, **308B**, 347–356.
25 H. Ehrlich, M. Krautter, T. Hanke, P. Simon, C. Knieb, S. Heinemann and H. Worch, *J. Exp. Zool. Part B Mol. Dev. Evol.*, 2007, **308B**, 473–483.
26 M. Wysokowski, M. Motylenko, V. V. Bazhenov, D. Stawski, I. Petrenko, A. Ehrlich, T. Behm, Z. Kljajic, A. L. Stelling, T. Jesionowski and H. Ehrlich, *Front. Mater. Sci.*, 2013, **7**, 248–260.
27 C. Klinger, S. Żółtowska-Aksamitowska, M. Wysokowski, M. V. Tsurkan, R. Galli, I. Petrenko, T. Machałowski, A. Ereskovsky, R. Martinović, L. Muzychka, O. B. Smolii, N. Bechmann, V. Ivanenko, P. J. Schupp, T. Jesionowski, M. Giovine, Y. Joseph, S. R. Bornstein, A. Voronkina and H. Ehrlich, *Mar. Drugs*, 2019, **17**, 131.
28 I. Dziedzic, A. Voronkina, M. Pajewska-Szmyt, M. Kotula, A. Kubiak, H. Meissner, T. Duminis and H. Ehrlich, *Mar. Drugs*, 2023, **21**, 334.
29 T. Duminis, M. Heljak, W. Święszkowski, A. Ereskovsky, I. Dziedzic, M. Nowicki, M. Pajewska-Szmyt, A. Voronkina, S. R. Bornstein and H. Ehrlich, *Mar. Drugs*, 2023, **21**, 463.
30 S. Hirano and R. Yamaguchi, *Biopolymers*, 1976, **15**, 1685–1691.
31 S. Hirano and Y. Ohe, *Agric. Biol. Chem.*, 1975, **39**, 1337–1338.
32 H. Saitô, R. Tabeta and S. Hirano, *Chem. Lett.*, 1981, **10**, 1479–1482.
33 L. Vachoud, N. Zydowicz and A. Domard, *Carbohydr. Res.*, 2000, **326**, 295–304.
34 L. Vachoud and A. Domard, *Biomacromolecules*, 2001, **2**, 1294–1300.
35 L. Vachoud, N. Zydowicz and A. Domard, *Carbohydr. Res.*, 1997, **302**, 169–177.
36 G. K. Moore and G. A. F. Roberts, *Int. J. Biol. Macromol.*, 1980, **2**, 73–77.
37 G. K. Moore and G. A. F. Roberts, *Int. J. Biol. Macromol.*, 1980, **2**, 78–80.
38 N. Isobe, M. Tsudome, R. Kusumi, M. Wada, K. Uematsu, S. Okada and S. Deguchi, *ACS Appl. Polym. Mater.*, 2020, **2**, 1656–1663.
39 K. Ohkawa, D. Cha, H. Kim, A. Nishida and H. Yamamoto, *Macromol. Rapid Commun.*, 2004, **25**, 1600–1605.
40 D. Carlström, *J. Biophys. Biochem. Cytol.*, 1957, **3**, 669–683.
41 P. W. Stephens, J. A. Kaduk, T. N. Blanton, D. R. Whitcomb, S. T. Misture and M. Rajeswaran, *Powder Diffr.*, 2012, **27**, 99–103.
42 X. Lin, L. Zhang and B. Duan, *Mater. Horizons*, 2021, **8**, 2503–2512.
43 D. Xu, J. Huang, D. Zhao, B. Ding, L. Zhang and J. Cai, *Adv. Mater.*, 2016, **28**, 5844–5849.
44 H. J. Kong, E. Wong and D. J. Mooney, *Macromolecules*, 2003, **36**, 4582–4588.
45 V. Normand, D. L. Lootens, E. Amici, K. P. Plucknett and P. Aymard, *Biomacromolecules*, 2000, **1**, 730–738.
46 N. E. Mushi, J. Kochumalayil, N. T. Cervin, Q. Zhou and L. A. Berglund, *ChemSusChem*, 2016, **9**, 989–995.
47 C. Chang, S. Chen and L. Zhang, *J. Mater. Chem.*, 2011, **21**, 3865.
48 N. Isobe, T. Komamiya, S. Kimura, U.-J. Kim and M. Wada, *Int. J. Biol. Macromol.*, 2018, **117**, 625–631.
49 A. Nakayama, A. Kakugo, J. P. Gong, Y. Osada, M. Takai, T. Erata and S. Kawano, *Adv. Funct. Mater.*, 2004, **14**, 1124–1128.
50 S. M. Paterson, Y. S. Casadio, D. H. Brown, J. A. Shaw, T. V Chirila and M. V Baker, *J. Appl. Polym. Sci.*, 2013, **127**, 4296–4304.
51 R. Aston, K. Sewell, T. Klein, G. Lawrie and L. Grøndahl, *Eur. Polym. J.*, 2016, **82**, 1–15.
52 Z. Kaberova, E. Karpushkin, M. Nevoralová, M. Vetrík, M. Šlouf and M. Dušková-Smrčková, *Polymers (Basel).*, 2020, **12**, 578.
53 O. Glatter and O. Kratky, *Small angle X-ray scattering*, Academic Press, New York, 1982.
54 G. Fagherazzi, *Acta Crystallogr. Sect. A Found. Crystallogr.*, 1983, **39**, 500–500.
55 P. Sikorski, R. Hori and M. Wada, *Biomacromolecules*, 2009, **10**, 1100–1105.
56 J. Ricka and T. Tanaka, *Macromolecules*, 1984, **17**, 2916–2921.
57 E. Vasheghani-Farahani, J. H. Vera, D. G. Cooper and M. E. Weber, *Ind. Eng. Chem. Res.*, 1990, **29**, 554–560.